Increased incidence of napkin-ring sign plaques on cervicocerebral computed tomography angiography associated with the risk of acute ischemic stroke occurrence

Wu, J.P.; Zou, Y.; Meng, X.; Fan, Z.Y.; Geest, R. van der; Cui, F.; ... ; Zhang, F.

EUROPEAN SOCIETY OF RADIOLOGY
European Radiology

COMPUTED TOMOGRAPHY

Increased incidence of napkin-ring sign plaques on cervicocerebral computed tomography angiography associated with the risk of acute ischemic stroke occurrence

Jingping Wu[1,2], Ying Zou[2], Xiao Meng[3], Zhaoyang Fan[4], Rob van der Geest[5], Fang Cui[6], Jianyong Li[6], Tengyuan Zhang[6] and Fan Zhang[1,2*]

Abstract

Objectives Carotid atherosclerosis plays an essential role in the occurrence of ischemic stroke. This study aimed to investigate whether a larger burden of napkin-ring sign (NRS) plaques on cervicocerebral computed tomography angiography (CTA) increased the risk of acute ischemic stroke (AIS).

Methods This retrospective, single-center, cross-sectional study enrolled patients with NRS plaques identified in the subclavian arteries, brachiocephalic trunk, carotid arterial system, and vertebrobasilar circulation on contrast-enhanced cervicocerebral CTA. Patients were divided into AIS and non-AIS groups based on imaging within 12 h of symptom onset. Univariate and multivariate logistic regression analyses were performed to determine the risk factor of AIS occurrence.

Results A total of 202 patients (66.72 years ± 8.97, 157 men) were evaluated. Plaques with NRS in each subject of the AIS group ($N = 98$) were significantly more prevalent than that in the control group ($N = 104$) (1.96 ± 1.17 vs 1.41 ± 0.62). In the AIS group, there were substantially more NRS plaques on the ipsilateral side than contralateral side (1.55 ± 0.90 vs. 0.41 ± 0.66). NRS located on the ipsilateral side of the AIS showed an area under the receiver curve (AUC) of 0.86 to identify ischemic stroke. NRS plaque amounts were an independent risk factor for AIS occurrence (odds ratio, 1.86) after adjusting for other factors.

Conclusions Increased incidence of napkin-ring sign plaques on cervicocerebral CTA was positively associated with AIS occurrence, which could aid in detecting asymptomatic atherosclerotic patients at high risk of AIS in routine screening or emergency settings.

Clinical relevance statement Napkin-ring sign plaque provides an important imaging target for estimating acute ischemic stroke risk and identifying high-risk patients in routine screening or emergency settings, so that timely anti-atherosclerotic therapy can be used for prevention.

Jingping Wu and Ying Zou contributed to the work equally and could be regarded as co-first authors.

*Correspondence:
Fan Zhang
fanzradiology@126.com
Full list of author information is available at the end of the article

Springer

Key Points

- *This cross-sectional study investigated the association between high-risk carotid artery plaques and acute ischemic stroke.*
- *Increased incidence of napkin-ring sign plaques on cervicocerebral computed tomography angiography is positively associated with acute ischemic stroke occurrence.*
- *Napkin-ring signs help identify risky patients prone to acute ischemic stroke to facilitate prevention.*

Keywords Ischemic stroke, Computed tomography angiography, Atherosclerosis

Introduction

Ischemic stroke accounts for 80% of all strokes [1] and is the second most common cause of death worldwide [2]. Approximately 20–30% of ischemic strokes and transient ischemic attacks (TIA) are caused by carotid atherosclerosis, which is a major contributor to cerebrovascular disease (CVD) [3–5]. Aortic atherosclerotic disease is also a possible source of cerebral emboli and can lead to ischemic stroke and TIA [6–8]. Previously, the degree of luminal stenosis was thought to strongly correlate with ischemic events. However, several studies have provided compelling evidence to the contrary [9–11]. Rupture-prone plaques and plaques with rapid progression are considered vulnerable, presenting with thin fibrous caps, intraplaque hemorrhage (IPH), lipid-rich necrotic cores (LRNC), and irregular plaque surfaces, which are prone to causing ischemic stroke and thrombotic complications independent of the degree of stenosis, providing a non-invasive imaging target for improving risk-stratification for ischemic events [12–14]. For example, non-stenotic carotid artery disease with high-risk plaque (HRP) features is associated with embolic stroke of undetermined source, accounting for 9–25% of ischemic strokes [15–17].

Several noninvasive imaging modalities are capable of detecting HRPs. Carotid vessel wall imaging using magnetic resonance imaging (MRI) is currently the most suitable imaging technique for characterizing HRP features [13, 18, 19], while a relatively long vessel wall imaging protocol renders the technique susceptible to motion artifacts and examination failure, particularly in unstable patients with stroke [20]. In contrast, computed tomography angiography (CTA) is a rapid imaging technique with superior robustness against patient motion [21]. It is more widely accessible as a noninvasive vascular imaging modality, particularly in an emergency setting [22]. It can also provide additional information on plaque characteristics in the extracranial and intracranial arteries. Additionally, CTA can detect and quantify multiple HRPs on different vessel beds, which was corroborated by histopathology and intravascular ultrasound [14, 18, 23–27].

An NRS arising from a central necrotic lipid core encircled by fibrous tissue was first identified in a coronary CTA study [28] as a HRP feature which could improve risk classification for adverse events and predict future major adverse cardiovascular events (MACE) [29–33]. Additionally, an NRS was identified as the strongest predictor of MACE [34]. NRS on CTA presents as a thin-cap fibroatheroma (TCFA), indicative of a plaque prone to rupture, and is prevalent in patients with acute cardiocerebral events [35]. TCFA plaques were more frequently involved in NRS than non-TCFA plaques [36]. The presence of plaques with NRS suggests advanced lesions with high specificity [34].

Previous studies have revealed the role of NRS plaques on the coronary artery while few studies have investigated the effect of NRS on the cervicocerebral arteries, particularly the association with ischemic stroke. We aimed to determine the associations between the burden of NRS plaques and acute ischemic stroke (AIS). We hypothesized that more NRS plaques would increase the risk of AIS occurrence, and the observation of NRS on routine CTA would provide an imaging tool to identify asymptomatic individuals at risk of AIS.

Materials and methods

Study population

This retrospective, single-center, cross-sectional study adhered to the Declaration of Helsinki and was approved by the Hospital's Medical Ethics Committee. Informed consent was obtained from all patients. Patients with symptoms or clinical suspicion of AIS who presented at our primary stroke center and underwent a cervicocerebral CTA examination between January 2019 and March 2022 were recruited. We retrieved patients with the keyword "cervicocerebral CTA" from the medical record system. The inclusion criteria were as follows: (1) observation of NRS plaques and (2) CTA of the head and neck extending from the aortic arch to the skull vertex, following standard protocols. The exclusion criteria were as follows: (1) prior carotid endarterectomy or stenting, which may cause restenosis due to the intimal damage [37, 38], leading to recurrent ischemic stroke and confounding the role of NRS plaques in AIS; (2) cardiac thrombus; (3) arterial occlusion in the vessel segment associated with ischemic stroke; (4) poor image quality

including the artifact and irregular scanning; (5) nonatherosclerotic lesion of the arteries, such as aneurysm, dissection, and moyamoya; (6) TIA (i.e., a brief episode of neurologic dysfunction which lasted less than 24 h). The recruited patients were divided into two groups according to the AIS diagnosis. AIS was diagnosed based on symptoms (e.g., paralysis, limb weakness, headache, and vomiting), along with imaging results from MRI within 12 h of symptom onset and non-enhanced CT, according to the American Heart Association or American College of Cardiology guidelines [39].

CTA protocols

Cervicocerebral CTA imaging was performed on dual-layer detector CT scanner (IQon Spectral; Phillips Healthcare). Patients were scanned from the aortic arch to the skull vertex in caudocranial and helical scan modes. The acquisition parameters were as follows: collimator width, 64 × 0.625 mm; tube voltage, 120 kVp; tube current control technology, automatic; rotation speed, 0.5 s/cycle; pitch, 0.969; rotation time, 0.27 s; reconstruction layer thickness, 0.9 mm; and isotropic imaging spatial resolution, 0.3 × 0.3 × 0.3 mm^3 in *x*, *y*, and *z* dimensions. Ultravist Solution (370 mg Iodine/mL; Bayer Healthcare) was injected through the antecubital vein as a contrast agent. The contrast-agent intelligent tracking threshold trigger technology was used to determine the enhanced scan time. The trigger point was set in the ascending aorta (attenuation threshold ranging from 100 to 120 Hounsfield units). For CTA acquisition, 60–80 mL of the contrast medium was injected at a rate of 3.5 mL/s.

CTA image analysis

After scanning, all CT data were transferred to a post-processing workstation (Philips Intelli Space Portal) for image analysis. Volume-rendered, maximum intensity projection, multiplanar reformatted, and curved planar reformatted images of the different segments of the measured arteries were reconstructed in the axial, coronal, and sagittal planes. Examples are shown in Fig. 2.

Quantitative and qualitative analyses of the images were performed using dedicated software (VesselMass, Leiden University Medical Center). The outer vessel wall, lumen, and low- and high-attenuation regions were manually traced in an axial slice, where the largest plaque burden was observed, and the contours were saved. An experienced radiologist with 10 years of experience in cervicocerebral CTA analyzed all the images and was blinded to the clinical information.

Previous pathological studies showed that atherosclerotic lesions are distributed across certain segments [40]. We selected the major segments intracranially and extracranially, including brachiocephalic trunk, bilateral subclavian arteries (Lsa and Rsa), bilateral common carotid artery bifurcation (Lbi and Rbi), bilateral common carotid artery (Lcca and Rcca), bilateral internal carotid arteries (C1–C6) and bilateral cerebral anterior, middle and posterior arteries, vertebral cerebral artery (LACA1–4 and RACA1–4, LMCA1–4 and RMCA1–4, LPCA1–4 and RPCA1–4, LV1–4 and RV1–4), and the basilar artery (BA).

NRS on CTA was defined according to a previously published study as follows: an inner hypodense core surrounded by an outer high-density ring of no more than 130 Hounsfield units [34]. Additionally, the plaques under investigation were not near calcification, to avoid a beam-hardening artifact [31]. In multiple (at least three cross-sectional) images along the plaque, the CT attenuation values of the plaque were measured through a 5-pixel region of interest at multiple sites in the plaque and averaged [33]. The remodeling index (RI) was calculated as the cross-sectional area of the largest stenosis divided by the average of the cross-sectional areas of the proximal and distal reference segments (≤ 10 mm) in the location of the NRS with the largest plaque burden, and an RI ≥ 1.05 indicates PR [41].

Ascertainment of covariates

Clinical factors adjusted for post-ablation AF recurrence are shown in Table 4. The International Society of Hypertension (ISH) defines hypertension as a systolic blood pressure ≥ 140 mmHg and diastolic blood pressure ≥ 90 mmHg in the absence of anti-hypertensive medication. According to the American Diabetes Association (ADA), diabetes is diagnosed based on symptoms such as polyuria, excessive drinking, unexplained weight loss, one random venous plasma glucose concentration ≥ 11.1 mmol/L, and fasting blood glucose concentration ≥ 7.0 mmol/L or 2-h glucose concentration ≥ 11.1 mmol/L. Hyperlipidemia is determined by triacylglycerol (TG) > 1.7 mmol/L and total cholesterol (TC) > 5.72 mmol/L, as per the Chinese guidelines for the prevention and treatment of adult dyslipidemia (Revised Version from 2016). The World Health Organization (WHO) defines smoking as consistent or cumulative smoking for at least 6 months, while drinking is defined as men consuming more than 60 g of pure alcohol per day and women consuming more than 40 g daily.

Statistical analysis

Statistical analyses were performed using commercially available software (SPSS26.0, SPSS; GraphPad Prism version 9.0, GraphPad Software). Continuous variables were expressed as means ± standard deviation, and categorical variables were expressed as frequencies or percentages. The one-sample Kolmogorov–Smirnov test was used

to check the assumption of a normal distribution. Continuous variables were compared between groups using either Student's *t*-test or the Mann–Whitney *U* test (for two groups, as appropriate). The chi-square test was used to analyze categorical variables. Univariate logistic regression analysis included variables related to AIS such as age, sex, BMI, LDL, HDL, CAD, hypertension, diabetes mellitus, hyperlipidemia, and medication (antiplatelet drugs, statins, ACEI/ARB, β-blockers). We computed the VIF (variance inflation factor) and found a collinearity between LDL and TG (VIF > 10). Therefore, we used stepwise regression including all the variance to select significant variance and avoid collinearity. Receiver-operating characteristics (ROC) curves were analyzed to evaluate the capacity of NRS for identifying stroke. A directed acyclic graph was made through the official website (http://www.dagitty.net/). Statistical significance was set at a two-tail probability value of $p < 0.05$.

Results

Patient characteristics

A total of 202 patients were enrolled in the final analysis (Fig. 1), including 98 (74 men, 75.51%) with AIS and 104 (83 men, 79.81%) without AIS. The baseline characteristics of the patients are summarized in Table 1. The participants in the AIS group were significantly older than those in the control group (68.00 ± 9.36 vs. 65.51 ± 8.46, $p = 0.042$). There were no statistically significant differences between the two groups in terms of sex, body mass index (BMI), cardiovascular risk factors, or medications.

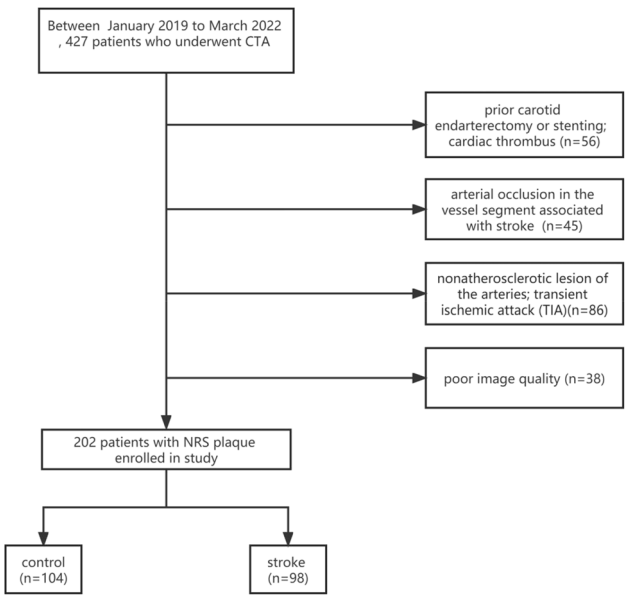

Fig. 1 Study flow diagram. Abbreviation: NRS, napkin ring sign

Table 1 Baseline clinical characteristics related to patients for stroke and control groups

	Stroke ($N = 98$)	Control ($N = 104$)	*p* value
Age (years)	68.00 ± 9.36	65.51 ± 8.46	0.042
Male, *n* (%)	74 (75.51%)	83 (79.81%)	0.463
BMI (kg/m^2)	24.28 ± 2.94	24.85 ± 2.14	0.288
LDL (mmol/L)	2.64 ± 1.05	2.35 ± 0.83	0.054
HDL (mmol/L)	1.08 ± 0.25	1.12 ± 0.27	0.270
TG (mmol/L)	4.11 ± 1.16	3.83 ± 0.99	0.085
TC (mmol/L)	1.47 ± 0.76	1.47 ± 0.93	0.638
CAD, *n* (%)	21 (21.43%)	30 (28.85%)	0.225
Hypertension, *n* (%)	60 (61.22%)	55 (52.88%)	0.232
Diabetes mellitus, *n* (%)	25 (25.51%)	31 (29.81%)	0.495
Hyperlipidemia, *n* (%)	17 (17.35%)	21 (20.19%)	0.605
Current smoking, *n* (%)	29 (29.59%)	22 (21.15%)	0.168
Drinking, *n* (%)	34 (34.69%)	25 (24.04%)	0.096
Antiplatelet drugs, *n* (%)	46 (46.94%)	54 (51.92%)	0.479
Statins, *n* (%)	37 (37.76%)	22 (21.15%)	0.010
β-Blockers, *n* (%)	4 (4.08%)	8 (7.69%)	0.278
ACEI/ARB, *n* (%)	16 (16.33%)	13 (12.50%)	0.438

Continuous values are expressed as mean ± SD, and categorical variables are expressed as frequencies (percentage)

Abbreviations: *BMI*, body mass index; *LDL*, low-density lipoprotein; *HDL*, high-density lipoprotein; *TG*, triglycerides; *TC*, total cholesterol; *CAD*, coronary artery disease; *ACEI*, angiotensin-converting enzyme inhibitor; *ARB*, angiotensin receptor blockers

Compared with the control group, a higher percentage of patients in the AIS group used statins (Fig. 2).

Table 2 summarizes the NRS characteristics of all patients as well as the ipsilateral and contralateral sides of the ischemic stroke. Each individual in the AIS group had significantly more total NRS than the control group (1.96 ± 1.17 vs. 1.41 ± 0.62, $p = 0.001$). Moreover, the ipsilateral side observed a higher NRS amount compared with the contralateral side per subject (1.55 ± 0.90 vs. 0.41 ± 0.66, $p < 0.001$). The plaque area was larger in the AIS group than the control (24.21 ± 24.22 vs. 10.74 ± 8.74 mm^2, $p < 0.001$). The average plaque area in the ipsilateral side was not significantly different from the contralateral side (11.14 ± 8.27 vs. 14.69 ± 12.16 mm^2, $p = 0.156$). The plaque in the AIS group had a higher PR than that in the control group (23/98 vs. 4/104, $p < 0.001$), as well as in the ipsilateral and contralateral sides (23/98 vs. 4/98, $p < 0.001$). After adjusting for confounding factors, multivariate logistic regression analysis revealed that the total NRS amount increased the risk of AIS (odds ratio 1.86, 95%CI: 1.30–2.65, $p = 0.001$) (Table 4). The average CT attenuation within the NRS plaque was lower on the ipsilateral side compared to the contralateral side (28.42 ± 12.11 vs. 37.66 ± 18.89 Hounsfield units, $p = 0.03$).

Table 3 reports the spatial distribution patterns of NRS between AIS and the control group as well as ipsilateral

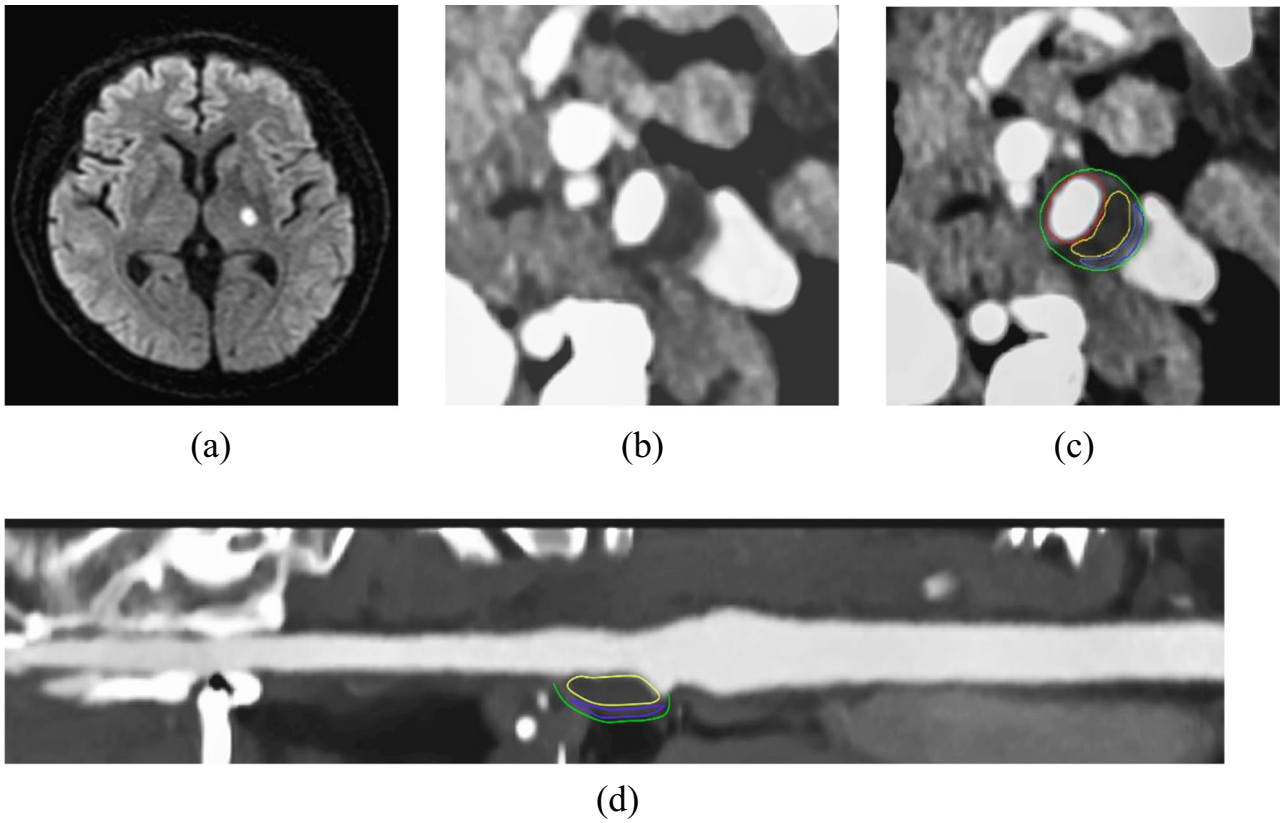

Fig. 2 A 69-year-old man diagnosed with ischemic stroke in the left basal ganglia region (shown in the diffusion-weighted images, **a**) with numbness and weakness in the right extremities had a plaque with NRS at the left common carotid artery identified on CTA (**b**, **c**). The yellow round demonstrates the low attenuation area of the plaque surrounded by a high-attenuation rim (purple round), and the blue area represents the lumen filled with contrast. The reconstruction image (MPR) was shown as picture (**d**)

Table 2 Comparison of the plaque with napkin-ring sign counts between stroke and control groups as well as ipsilateral and contralateral sides in the stroke group

	Stroke ($N=98$)	Control ($N=104$)	*p* value	Ipsilateral	Contralateral	*p* value
NRS counts	1.96 ± 1.17	1.41 ± 0.62	0.001	1.55 ± 0.90	0.41 ± 0.66	< 0.001
NRS area (mm^2)	24.21 ± 24.22	10.74 ± 8.74	< 0.001	11.14 ± 8.27	14.69 ± 12.16	0.156
Positive remodeling (> 1.05)	23 (8.16%)	4 (3.85%)	< 0.001	23 (23.47%)	10 (10.20%)	0.013
CT attenuation value (HU)	_	_	_	28.42 ± 12.11	37.66 ± 18.89	0.030

Table 3 Comparison of the plaque with napkin-ring sign counts between stroke and control groups as well as ipsilateral and contralateral sides in the stroke group in different segments

	Stroke ($N=98$)	Control ($N=104$)	*p* value	Ipsilateral	Contralateral	*p* value
Subclavian artery, bilateral	0.20 ± 0.41	0.11 ± 0.34	0.035	0.18 ± 0.39	0.01 ± 0.10	< 0.001
Brachiocephalic trunk	0.16 ± 0.37	0.08 ± 0.27	0.059	0.16 ± 0.37	0	< 0.001
Common carotid artery, bilateral	0.90 ± 0.83	0.66 ± 0.71	0.049	0.60 ± 0.59	0.29 ± 0.50	< 0.001
Carotid bifurcation, bilateral	0.39 ± 0.55	0.33 ± 0.55	0.337	0.33 ± 0.53	0.10 ± 0.30	< 0.001
C1, bilateral	0.30 ± 0.50	0.24 ± 0.45	0.446	0.26 ± 0.46	0.02 ± 0.14	< 0.001
Other segments	0	0	N/A	0	0	N/A

The distribution characteristics of the plaques with napkin-ring sign on the carotid artery

and contralateral sides to the AIS. Corresponding spatial distribution patterns of the plaques with NRS are further summarized in Fig. 3. For diagnosing AIS, the total NRS and ipsilateral NRS had AUCs of 0.62 and 0.86, respectively. ROC analysis determined that a total NRS ≥ 2 was the optimal cutoff threshold to diagnose AIS (Fig. 4).

The directed acyclic graph presented AIS as a dependent variable and enrolled other variables characterized in two groups: independent (NRS account, LDL, and statins) and confounding variables (age, sex, BMI, HDL, TG, TC, CAD, hypertension, diabetes mellitus, hyperlipidemia, current smoking, drinking, antiplatelet drugs, β-blockers, and ACEI/ARB), which were verified by our results. Statin was classified as an independent variable to avoid it affecting LDL, HDL, TC, and TG (Fig. 5).

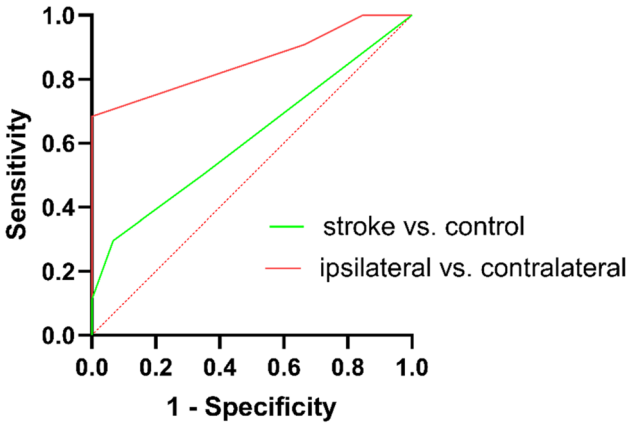

Fig. 4 Receiver operating characteristic (ROC) analysis showed diagnostic characteristics of napkin-ring sign plaques (NRS) between the stroke and control groups, as well as ipsilateral and contralateral sides to the stroke group

Discussion

Our study revealed that increased incidence of NRS, as an imaging marker of vulnerable plaques on cervicocerebral CTA, is a risk factor for ischemic stroke occurrence. The early observation of NRS on CTA may help identify patients who are prone to AIS and allow early anti-atherosclerotic treatment to prevent ischemic cerebral events.

NRS in coronary plaques was identified as TCFA, a precursor lesion prone to rupture [28, 42] by pathology and invasive optical coherence tomography [33, 43]. A ring-like enhancement sign of plaque on CCTA was found in 25% of culprit lesions in patients with acute coronary syndrome (ACS) [44]. Advanced atherosclerotic lesions identified by pathological evaluation were observed in all plaques with NRS [34]. The ring-like enhancement reflects the high-attenuation rim of the NRS. Extrapolating from the existing evidence on coronary arteries, ring-like enhancement indicates highly active vasa vasorum neovascularization by histopathological examination, which usually happens in advanced lesions and is associated with vulnerable plaques [45, 46]. The necrotic core activates macrophages that will secrete inflammatory factors. Neovascularization and inflammation are considered the main causes of atherosclerotic plaque vulnerability and rupture [47]. Therefore, NRS is potentially an imaging biomarker that reflects plaque susceptibility [45, 48].

Over the past few decades, few studies have mentioned the correlation between NRS on the carotid artery and cerebral events. The necrotic core is a predictive factor for ischemic stroke [13], and ignoring the high-attenuation rim indicates the normality of mistaking the NRS as a necrotic core, leading to misrepresentations of the clinical behavior of cerebrovascular diseases.

A prior study investigated whether plaques with NRS in the carotid artery were associated with acute myocardial infarction, and NRS was only observed in two individuals [49]. The small sample size was insufficient to assess

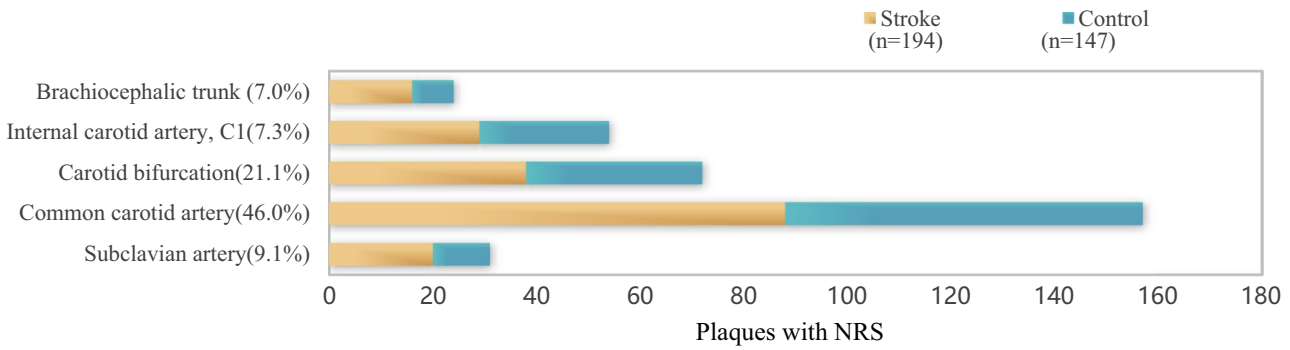

Fig. 3 The spatial distribution of the plaques with NRS between the stroke group and control group. Two types of color bar represent the NRS count at each vessel segment in two groups and the relative proportion to the total NRS count. A higher frequency of NRS was observed at the common carotid artery, followed by carotid bifurcation, subclavian artery, internal carotid artery, and brachiocephalic trunk, suggesting a predilection site for the plaque with NRS

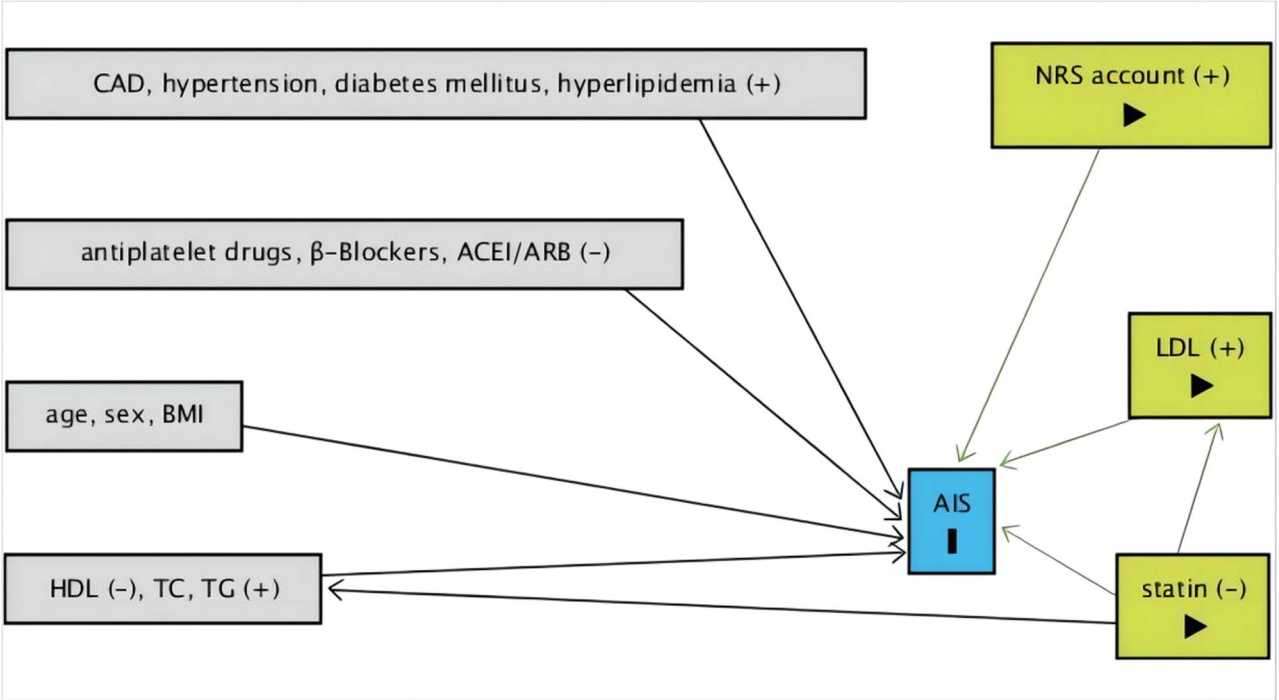

Fig. 5 Directed acyclic graph based on known associations. AIS as dependent variable; NRS account, LDL, and statins as independent variables; age, sex, BMI, HDL, TG, TC, CAD, hypertension, diabetes mellitus, hyperlipidemia, current smoking, drinking, antiplatelet drugs, β-blockers, and ACEI/ARB as confounding variables. "(+)" presents a positive association while "(-)" indicates negative. Abbreviations: NRS, napkin-ring sign; BMI, body mass index; LDL, low-density lipoprotein; HDL, high-density lipoprotein; TG, triglycerides; TC, total cholesterol; CAD, coronary artery disease; ACEI, angiotensin-converting enzyme inhibitor; ARB, angiotensin receptor blockers

Table 4 Univariable and multivariable logistic regression analyses to compare patients with stroke and the controls

	Univariable	**Multivariable**
	OR (95% CI) *p* value	**OR (95% CI) *p* value**
Age (years)	1.03 (1.00–1.07) 0.05	
Male, *n* (%)	1.28 (0.66–2.50) 0.46	
BMI (kg/m^2)	0.92 (0.82–1.02) 0.12	
LDL (mmol/L)	1.39 (1.03–1.89) 0.03	1.48 (1.06–2.06) 0.02
HDL (mmol/L)	0.62 (0.21–1.78) 0.37	
TG (mmol/L)	1.27 (0.98–1.66) 0.07	
TC (mmol/L)	0.99 (0.72–1.37) 0.97	
CAD, *n* (%)	1.49 (0.78–2.83) 0.23	
Hypertension, *n* (%)	0.71 (0.41–1.24) 0.23	
Diabetes mellitus, *n* (%)	1.24 (0.67–2.30) 0.50	
Hyperlipidemia, *n* (%)	1.21 (0.59–2.45) 0.61	
Current smoking, *n* (%)	1.57 (0.83–2.97) 0.17	
Drinking, n (%)	1.68 (0.91–3.10) 0.10	
Antiplatelet drugs, n (%)	1.22 (0.70–2.12) 0.48	
Statins, *n* (%)	0.44 (0.24–0.83) 0.01	0.42 (0.21–0.82) 0.01
β-Blockers, *n* (%)	0.51 (0.15–1.75) 0.29	
ACEI/ARB, *n* (%)	0.73 (0.33–1.61) 0.44	
Total amount	1.28 (0.66–2.50) 0.46	1.86 (1.30–2.65) 0.001

The results of the univariable and multivariate logistic regression models after adjusting for the influence of age, sex, BMI, CAD, hypertension, diabetes mellitus, LDL, HDL, TC, TG, current smoking, drinking, hyperlipidemia, and medications to observe the effect of total NRS amount on the incidence of ischemic stroke

Abbreviations: *OR*, odd ratio; *CI*, confidence interval

the distribution and frequency of NRS in the cervicocerebral arteries and to determine its role in ischemic events. Therefore, our study contributes to the current body of knowledge by focusing on plaques using NRS in the cervicocerebral arteries and demonstrating their connection with ischemic stroke. It has been shown that the total number of plaques with NRS is an independent indicator of ischemic stroke. We found that total NRS plaque ≥ 2 was a threshold to diagnose stroke, and that it might differ considerably in populations with different degrees of NRS. Additionally, our study found a higher prevalence of NRS on the ipsilateral side of patients with ischemic stroke than on the contralateral side. Most plaques in the extracranial arteries were found in the common carotid arteries, indicating a specific spatial pattern of NRS, and likely providing a potential sentinel point for the management of ischemic cerebral events. This study found no plaques with NRS in the small intracranial arteries, partly because of the blooming artifact on CT, which affects plaque assessment.

We discovered that NRS plaques on the ipsilateral side of the ischemic stroke showed more PR and lower attenuation than those on the contralateral side. Motoyama et al [50] concluded that the PR and low CT attenuation are important multi-detector CT imaging markers for vulnerable plaques. Higher atheroma volume or an advanced arterial

Table 5 Indicators of ROC analysis of total and ipsilateral NRS amounts to identify acute ischemic stroke

	AUC (95% CI)	Sensitivity (%)	Specificity (%)	Positive predictive value (%)	Negative predictive value (%)
Total NRS amounts	0.62 (0.54–0.68)	29.59%	93.27%	80.55%	58.45%
Ipsilateral NRS amounts	0.86 (0.80–0.90)	100%	67.35%	75.39%	100%

The results of ROC analysis of NRS amounts in identifying AIS

Abbreviations: *ROC*, receiver operating characteristic; *AUC*, area under curve

compensatory condition could increase endothelial dysfunction and become the proposed mechanisms of PR. Low attenuation plaque (LAP) is associated with an elevated risk of cardiovascular events and is a strong predictor of plaque rupture [31, 51]. It is reported that CT attenuation values were lower in plaques with NRS and unstable neovascularization rings worsened this process [33]. The distinct plaque density reflects different hemodynamic changes on the two sides of the carotid arteries in the same individual, leading to ischemic events (Tables 4 and 5).

Plaques with NRS showed larger areas in the AIS group than in the control group, consistent with the fact that plaques with large areas tend to be vulnerable to rupture [50]. According to previous invasive studies, a larger necrotic core in patients with coronary atherosclerosis increases the probability of plaque rupture [52]. In addition, an increased necrotic core area is an independent predictor of the presence of NRS [48]. Thus, it can be concluded that plaque size is correlated with adverse cardiocerebral events, and a larger plaque area with NRS increases the risk of ischemic stroke. However, the finding of an insignificantly smaller area on the ipsilateral side of the ischemic stroke suggested heterogeneity in the time and space of the formation and rupture of the plaques, and Kashiwagi et al also failed to find a difference in plaque area between TCFA and non-TCFA [45]. A single scan simply cannot describe the entire dynamic process of atherosclerosis, and further studies are required to confirm this hypothesis.

Our study had several limitations. First, we did not find plaques with NRS in the intracranial arteries or vertebrobasilar circulation on cervicocerebral CTA, mainly because of the limited resolution and blooming artifacts of CT. Second, the cross-sectional study design limited the inferences of causality by exploring the association between NRS scores and ischemic stroke at a particular time point. Third, this study represents a single-center, retrospective study of patients referred for CTA, which may have contributed to selection bias. The limited number of patients in our study suggests the necessity of a larger number of patients in a prospective study in the future to elucidate the prognostic value of the NRS for ischemic stroke and delineate how high-risk plaques develop during ischemic events. Evolving techniques such as black blood MRI or photon-counting detector CT could be helpful in detecting intracranial atherosclerotic disease in patients with unstable plaques.

In conclusion, our study suggests increased NRS plaques on cervicocerebral CTA are an independent and important risk factor for ischemic stroke occurrence, and the exploration of the NRS is promising as an imaging biomarker to provide insight into the risk for AIS.

Abbreviations

ACS	Acute coronary syndrome
AIS	Acute ischemic stroke
CTA	Computed tomography angiography
CVD	Cerebrovascular disease
HRP	High-risk plaques
LAP	Low attenuation plaque
MACE	Major adverse cardiovascular events
NRS	Napkin-ring sign
PR	Positive remodeling
TCFA	Thin-cap fibroatheroma
TIA	Transient ischemic attack

Acknowledgements
We would like to thank all the patients who agreed to participate in this study.

Funding
This work is supported by the Key R&D program of Hainan Province (ZDYF2019169), Natural Science Foundation of Hainan Province (822RC738), and Sanya University Talent Introduction Project (USYRC22-05).

Declarations

Guarantor
The scientific guarantor of this publication is Fan Zhang.

Conflict of interest
The authors of this manuscript declare no relationships with any companies, whose products or services may be related to the subject matter of the article.

Statistics and biometry
No complex statistical methods were necessary for this paper.

Informed consent
Written informed consent was obtained from all subjects (patients) in this study.

Ethical approval
Institutional Review Board approval was obtained. This study has been approved by our institutional Medical Ethical Committee of Hainan Hospital of PLA General Hospital.

Study subjects or cohorts overlap
Study subjects or cohorts have not been previously reported.

Methodology

- retrospective
- cross-sectional study
- performed at one institution

Author details
[1]The Second School of Clinical Medicine, Southern Medical University, Guangzhou, China. [2]Department of Radiology, Hainan Hospital of PLA General Hospital, Sanya, China. [3]Department of Nutrition, School of Public Health, Sun Yat-Sen University, Guangzhou, China. [4]Department of Radiology, University of Southern California, Los Angeles, CA, USA. [5]Department of Radiology, Leiden University Medical Center, Leiden, The Netherlands. [6]Department of Neurology, Hainan Hospital of PLA General Hospital, Sanya, China.

Received: 5 April 2023 Revised: 6 September 2023 Accepted: 18 September 2023
Published online: 25 November 2023

References

1. Meyers PM, Schumacher HC, Connolly ES Jr, Heyer EJ, Gray WA, Higashida RT (2011) Current status of endovascular stroke treatment. Circulation 123:2591–2601. https://doi.org/10.1161/circulationaha.110.971564
2. Feigin VL, Nichols E, Alam T et al (2019) Global, regional, and national burden of neurological disorders, 1990–2016: a systematic analysis for the Global Burden of Disease Study 2016. Lancet Neurol 18:459–480. https://doi.org/10.1016/s1474-4422(18)30499-x
3. Song P, Fang Z, Wang H et al (2020) Global and regional prevalence, burden, and risk factors for carotid atherosclerosis: a systematic review, meta-analysis, and modelling study. Lancet Glob Health 8:e721–e729. https://doi.org/10.1016/s2214-109x(20)30117-0
4. Tan AP, Taneja M, Seah BH, Leong HN, Venketasubramanian N (2014) Acute free-floating carotid artery thrombus causing stroke in a young patient: unique etiology and management using endovascular approach. J Stroke Cerebrovasc Dis 23:e437–e439. https://doi.org/10.1016/j.jstrokecerebrovasdis.2014.05.005
5. Rothwell PM, Eliasziw M, Gutnikov SA, Warlow CP, Barnett HJ (2004) Endarterectomy for symptomatic carotid stenosis in relation to clinical subgroups and timing of surgery. Lancet 363:915–924. https://doi.org/10.1016/s0140-6736(04)15785-1
6. Amarenco P, Cohen A, Tzourio C et al (1994) Atherosclerotic disease of the aortic arch and the risk of ischemic stroke. N Engl J Med 331:1474–1479. https://doi.org/10.1056/nejm199412013312202
7. Guidoux C, Mazighi M, Lavallée P et al (2013) Aortic arch atheroma in transient ischemic attack patients. Atherosclerosis 231:124–128. https://doi.org/10.1016/j.atherosclerosis.2013.08.025
8. Viedma-Guiard E, Guidoux C, Amarenco P, Meseguer E (2020) Aortic sources of embolism. Front Neurol 11:606663. https://doi.org/10.3389/fneur.2020.606663
9. Freilinger TM, Schindler A, Schmidt C et al (2012) Prevalence of nonstenosing, complicated atherosclerotic plaques in cryptogenic stroke. JACC Cardiovasc Imaging 5:397–405. https://doi.org/10.1016/j.jcmg.2012.01.012
10. Gupta A, Gialdini G, Lerario MP et al (2015) Magnetic resonance angiography detection of abnormal carotid artery plaque in patients with cryptogenic stroke. J Am Heart Assoc 4:e002012. https://doi.org/10.1161/jaha.115.002012
11. Inzitari D, Eliasziw M, Gates P et al (2000) The causes and risk of stroke in patients with asymptomatic internal-carotid-artery stenosis. North American Symptomatic Carotid Endarterectomy Trial Collaborators. N Engl J Med 342:1693–1700. https://doi.org/10.1056/nejm200006083422302
12. Naghavi M, Libby P, Falk E et al (2003) From vulnerable plaque to vulnerable patient: a call for new definitions and risk assessment strategies: Part I. Circulation 108:1664–1672. https://doi.org/10.1161/01.Cir.0000087480.94275.97
13. Saba L, Saam T, Jäger HR et al (2019) Imaging biomarkers of vulnerable carotid plaques for stroke risk prediction and their potential clinical implications. Lancet Neurol 18:559–572. https://doi.org/10.1016/s1474-4422(19)30035-3
14. Baradaran H, Gupta A (2020) Carotid Vessel Wall Imaging on CTA. AJNR Am J Neuroradiol 41:380–386. https://doi.org/10.3174/ajnr.A6403
15. Hart RG, Catanese L, Perera KS, Ntaios G, Connolly SJ (2017) Embolic stroke of undetermined source: a systematic review and clinical update. Stroke 48:867–872. https://doi.org/10.1161/strokeaha.116.016414
16. Goyal M, Singh N, Marko M et al (2020) Embolic stroke of undetermined source and symptomatic nonstenotic carotid disease. Stroke 51:1321–1325. https://doi.org/10.1161/strokeaha.119.028853
17. Tao L, Li XQ, Hou XW et al (2021) Intracranial atherosclerotic plaque as a potential cause of embolic stroke of undetermined source. J Am Coll Cardiol 77:680–691. https://doi.org/10.1016/j.jacc.2020.12.015
18. Saba L, Antignani PL, Gupta A et al (2022) International Union of Angiology (IUA) consensus paper on imaging strategies in atherosclerotic carotid artery imaging: from basic strategies to advanced approaches. Atherosclerosis 354:23–40. https://doi.org/10.1016/j.atherosclerosis.2022.06.1014
19. Saba L, Yuan C, Hatsukami TS et al (2018) Carotid artery wall imaging: perspective and guidelines from the ASNR Vessel Wall Imaging Study Group and Expert Consensus Recommendations of the American Society of Neuroradiology. AJNR Am J Neuroradiol 39:E9-e31. https://doi.org/10.3174/ajnr.A5488
20. Boussel L, Herigault G, de la Vega A, Nonent M, Douek PC, Serfaty JM (2006) Swallowing, arterial pulsation, and breathing induce motion artifacts in carotid artery MRI. J Magn Reson Imaging 23:413–415. https://doi.org/10.1002/jmri.20525
21. Kim JJ, Dillon WP, Glastonbury CM, Provenzale JM, Wintermark M (2010) Sixty-four-section multidetector CT angiography of carotid arteries: a systematic analysis of image quality and artifacts. AJNR Am J Neuroradiol 31:91–99. https://doi.org/10.3174/ajnr.A1768
22. Amin HP, Madsen TE, Bravata DM et al (2023) Diagnosis, workup, risk reduction of transient ischemic attack in the emergency department setting: a scientific statement from the American Heart Association. Stroke. https://doi.org/10.1161/str.0000000000000418
23. Oliver TB, Lammie GA, Wright AR et al (1999) Atherosclerotic plaque at the carotid bifurcation: CT angiographic appearance with histopathologic correlation. AJNR Am J Neuroradiol 20:897–901
24. Chrencik MT, Khan AA, Luther L et al (2019) Quantitative assessment of carotid plaque morphology (geometry and tissue composition) using computed tomography angiography. J Vasc Surg 70:858–868. https://doi.org/10.1016/j.jvs.2018.11.050
25. Varrassi M, Sferra R, Gravina GL et al (2019) Carotid artery plaque characterization with a wide-detector computed tomography using a dedicated post-processing 3D analysis: comparison with histology. Radiol Med 124:795–803. https://doi.org/10.1007/s11547-019-01026-8
26. Tanaka A, Shimada K, Yoshida K et al (2008) Non-invasive assessment of plaque rupture by 64-slice multidetector computed tomography–comparison with intravascular ultrasound. Circ J 72:1276–1281. https://doi.org/10.1253/circj.72.1276
27. Voros S, Rinehart S, Qian Z et al (2011) Coronary atherosclerosis imaging by coronary CT angiography: current status, correlation with intravascular interrogation and meta-analysis. JACC Cardiovasc Imaging 4:537–548. https://doi.org/10.1016/j.jcmg.2011.03.006
28. Maurovich-Horvat P, Hoffmann U, Vorpahl M, Nakano M, Virmani R, Alkadhi H (2010) The napkin-ring sign: CT signature of high-risk coronary plaques? JACC Cardiovasc Imaging 3:440–444. https://doi.org/10.1016/j.jcmg.2010.02.003
29. Senoner T, Plank F, Barbieri F et al (2020) Added value of high-risk plaque criteria by coronary CTA for prediction of long-term outcomes. Atherosclerosis 300:26–33. https://doi.org/10.1016/j.atherosclerosis.2020.03.019
30. Otsuka K, Fukuda S, Tanaka A et al (2013) Napkin-ring sign on coronary CT angiography for the prediction of acute coronary syndrome. JACC Cardiovasc Imaging 6:448–457. https://doi.org/10.1016/j.jcmg.2012.09.016
31. Feuchtner G, Kerber J, Burghard P et al (2017) The high-risk criteria low-attenuation plaque <60 HU and the napkin-ring sign are the most powerful predictors of MACE: a long-term follow-up study. Eur Heart J Cardiovasc Imaging 18:772–779. https://doi.org/10.1093/ehjci/jew167

32. Yoon SH, Kim E, Jeon Y et al (2020) Prognostic value of coronary CT angiography for predicting poor cardiac outcome in stroke patients without known cardiac disease or chest pain: the Assessment of Coronary Artery Disease in Stroke Patients Study. Korean J Radiol 21:1055–1064. https://doi.org/10.3348/kjr.2020.0103
33. Kashiwagi M, Tanaka A, Shimada K et al (2013) Distribution, frequency and clinical implications of napkin-ring sign assessed by multidetector computed tomography. J Cardiol 61:399–403. https://doi.org/10.1016/j.jjcc.2013.01.004
34. Maurovich-Horvat P, Schlett CL, Alkadhi H et al (2012) The napkin-ring sign indicates advanced atherosclerotic lesions in coronary CT angiography. JACC Cardiovasc Imaging 5:1243–1252. https://doi.org/10.1016/j.jcmg.2012.03.019
35. Jang IK, Tearney GJ, MacNeill B et al (2005) In vivo characterization of coronary atherosclerotic plaque by use of optical coherence tomography. Circulation 111:1551–1555. https://doi.org/10.1161/01.Cir.0000159354.43778.69
36. Ito T, Terashima M, Kaneda H et al (2011) Comparison of in vivo assessment of vulnerable plaque by 64-slice multislice computed tomography versus optical coherence tomography. Am J Cardiol 107:1270–1277. https://doi.org/10.1016/j.amjcard.2010.12.036
37. Dai Z, Xu G (2017) Restenosis after carotid artery stenting. Vascular 25:576–586. https://doi.org/10.1177/1708538117706273
38. Bonati LH, Ederle J, McCabe DJ et al (2009) Long-term risk of carotid restenosis in patients randomly assigned to endovascular treatment or endarterectomy in the Carotid and Vertebral Artery Transluminal Angioplasty Study (CAVATAS): long-term follow-up of a randomised trial. Lancet Neurol 8:908–917. https://doi.org/10.1016/s1474-4422(09)70227-3
39. Mulder MJ, van Oostenbrugge RJ, Dippel DW (2015) Letter by Mulder et al regarding article, "2015 AHA/ASA Focused Update of the 2013 Guidelines for the Early Management of Patients With Acute Ischemic Stroke Regarding Endovascular Treatment: A Guideline for Healthcare Professionals From the American Heart Association/American Stroke Association." Stroke 46:e235. https://doi.org/10.1161/strokeaha.115.010913
40. Helgason CM, Wolf PA (1997) American Heart Association Prevention Conference IV: prevention and rehabilitation of stroke: executive summary. Circulation 96:701–707. https://doi.org/10.1161/01.cir.96.2.701
41. Ma N, Jiang WJ, Lou X et al (2010) Arterial remodeling of advanced basilar atherosclerosis: a 3-Tesla MRI study. Neurology 75:253–258. https://doi.org/10.1212/WNL.0b013e3181e8e714
42. Virmani R, Burke AP, Farb A, Kolodgie FD (2006) Pathology of the vulnerable plaque. J Am Coll Cardiol 47:C13-18. https://doi.org/10.1016/j.jacc.2005.10.065
43. Cheruvu PK, Finn AV, Gardner C et al (2007) Frequency and distribution of thin-cap fibroatheroma and ruptured plaques in human coronary arteries: a pathologic study. J Am Coll Cardiol 50:940–949. https://doi.org/10.1016/j.jacc.2007.04.086
44. Pflederer T, Marwan M, Schepis T et al (2010) Characterization of culprit lesions in acute coronary syndromes using coronary dual-source CT angiography. Atherosclerosis 211:437–444. https://doi.org/10.1016/j.atherosclerosis.2010.02.001
45. Kashiwagi M, Tanaka A, Kitabata H et al (2009) Feasibility of noninvasive assessment of thin-cap fibroatheroma by multidetector computed tomography. JACC Cardiovasc Imaging 2:1412–1419. https://doi.org/10.1016/j.jcmg.2009.09.012
46. Gössl M, Versari D, Hildebrandt HA et al (2010) Segmental heterogeneity of vasa vasorum neovascularization in human coronary atherosclerosis. JACC Cardiovasc Imaging 3:32–40. https://doi.org/10.1016/j.jcmg.2009.10.009
47. Dunmore BJ, McCarthy MJ, Naylor AR, Brindle NP (2007) Carotid plaque instability and ischemic symptoms are linked to immaturity of microvessels within plaques. J Vasc Surg 45:155–159. https://doi.org/10.1016/j.jvs.2006.08.072
48. Seifarth H, Schlett CL, Nakano M et al (2012) Histopathological correlates of the napkin-ring sign plaque in coronary CT angiography. Atherosclerosis 224:90–96. https://doi.org/10.1016/j.atherosclerosis.2012.06.021
49. Mosleh W, Adib K, Natdanai P et al (2017) High-risk carotid plaques identified by CT-angiogram can predict acute myocardial infarction. Int J Cardiovasc Imaging 33:561–568. https://doi.org/10.1007/s10554-016-1019-5
50. Motoyama S, Sarai M, Harigaya H et al (2009) Computed tomographic angiography characteristics of atherosclerotic plaques subsequently resulting in acute coronary syndrome. J Am Coll Cardiol 54:49–57. https://doi.org/10.1016/j.jacc.2009.02.068
51. Nakanishi K, Fukuda S, Shimada K et al (2012) Non-obstructive low attenuation coronary plaque predicts three-year acute coronary syndrome events in patients with hypertension: multidetector computed tomographic study. J Cardiol 59:167–175. https://doi.org/10.1016/j.jjcc.2011.11.010
52. Ino Y, Kubo T, Tanaka A et al (2011) Difference of culprit lesion morphologies between ST-segment elevation myocardial infarction and non-ST-segment elevation acute coronary syndrome: an optical coherence tomography study. JACC Cardiovasc Interv 4:76–82. https://doi.org/10.1016/j.jcin.2010.09.022

Publisher's Note